

Laboratory calibration of a MEMS accelerometer sensor

Irina Georgieva, Clemens Hofreither, Teodora Ilieva,
Tihomir Ivanov, Svetoslav Nakov

1. Introduction

Nowadays, systems, using microelectromechanical systems (MEMS) sensors (e.g. accelerometers, gyroscopes, etc.) find more and more applications. For instance, they are used for video stabilization, mobile applications and many other things. Among the reasons for their wide use is the fact that they are very cheap and have miniature size (usually less than $10 \times 10 \times 5$ mm) and consume little power. However, there are a lot of unexplored fields (like navigation) where they could be used once the necessary mathematical knowledge is developed. For further information, see for example [4].

In the present work we address MEMS accelerometers in particular. There are many sources of error that affect their behaviour [4]. In this report, we present two mathematical models and associated algorithms for calibrating the device, i.e. compensating for the constant bias error (the offset of its output signal, when the device does not undergo any acceleration), scaling errors (the deviation of the accelerometer's scale from the unit we want to use, like m/s^2) and nonorthogonality of the axis.

2. Approach 1

This approach was studied by Teodora Ilieva, Tihomir Ivanov and Svetoslav Nakov.

We have a system, consisting of three accelerometers, that measure the linear acceleration in three “almost” orthogonal directions. We shall assume that the angle between each two of those directions is $90^\circ \pm 2\%$ [5]. The relationship between accelerometer's outputs and the measured acceleration can be well modeled as a linear function [1]. In Subsection 2 we present the calibration algorithm. Similar approach to the problem is proposed, e.g., in [2], [3] (see also the references within those papers). There a six-parameter and a nine-parameter linear

models are developed for calibrating the device. Both of those approaches use an orthogonal coordinate system, with respect to which the corresponding analysis is carried. We study the problem by working in the coordinate system defined by the directions in which the accelerometers measure linear acceleration. We find this to be the more natural way and, thus, simplifying the analysis. Also, an usual thing to do is to approximate the sine and the cosine functions of small angles with the respective angles (which leads to the linearity of the aforementioned models). We do not use this approximation in order to obtain maximal accuracy in the model.

In Subsection 3 we study computationally the error that can be caused by not considering the non-orthogonality of the axis. We show that even small deviations in the directions of the accelerometers can lead to catastrophic error in the estimated position of the body within a few seconds of integrating.

2.1. Mathematical model describing the relationship between the measured and the real values of the acceleration

Let \hat{a}_x , \hat{a}_y and \hat{a}_z be the real values that the accelerometers show and a_x , a_y and a_z be the corresponding calibrated values of the acceleration in the x , y and z directions, respectively, with \vec{e}_1 , \vec{e}_2 and \vec{e}_3 being unit vectors in those directions. We use the following model to calibrate the accelerometers [1]:

$$(1) \quad \begin{aligned} a_x &= (\hat{a}_x - s_1)/b_1 \\ a_y &= (\hat{a}_y - s_2)/b_2, \\ a_z &= (\hat{a}_z - s_3)/b_3 \end{aligned}$$

where s_1 , s_2 , s_3 (which we call shifts) and b_1 , b_2 , b_3 (which we call scaling coefficients) are yet to be determined. In matrix form (1) can be written as

$$\underbrace{\begin{bmatrix} a_x \\ a_y \\ a_z \end{bmatrix}}_{\mathbf{a}} = \underbrace{\begin{bmatrix} 1/b_1 & 0 & 0 \\ 0 & 1/b_2 & 0 \\ 0 & 0 & 1/b_3 \end{bmatrix}}_T \underbrace{\begin{bmatrix} \hat{a}_x \\ \hat{a}_y \\ \hat{a}_z \end{bmatrix}}_{\hat{\mathbf{a}}} - \underbrace{\begin{bmatrix} s_1/b_1 \\ s_2/b_2 \\ s_3/b_3 \end{bmatrix}}_s.$$

Using the introduced notation, we obtain the equation

$$(2) \quad \mathbf{a} = T\hat{\mathbf{a}} - \mathbf{s}$$

Proposition 1. *If we assume that the axis of the accelerometers are orthogonal, then the acceleration is*

$$a_{orth} := \sqrt{a_x^2 + a_y^2 + a_z^2}$$

Proof. The proof is obvious, using the fact that the sum of the squares of the directional cosines is 1. \square

Since the axis are not orthogonal, let us denote the angles between the axis as follows (see Fig.1):

$$(3) \quad \phi := \angle(Ox, Oy), \quad \psi := \angle(Ox, Oz), \quad \theta := \angle(Oy, Oz)$$

Let \vec{a} be an arbitrary acceleration acting on the sensor. Let $\overline{a_x}$, $\overline{a_y}$ and $\overline{a_z}$ be the affine projections of \vec{a} onto the x , y and z axis, respectively. It is important to note that the measured values¹ of the acceleration in the x , y and z directions are not the affine projections of \vec{a} onto the axis. Let us denote (see Fig. 1)

$$\alpha := \angle(\vec{a}, \vec{e}_1), \beta := \angle(\vec{a}, \vec{e}_2), \gamma := \angle(\vec{a}, \vec{e}_3)$$

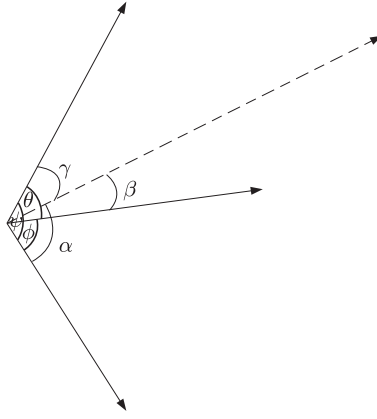


Figure 1: Acceleration vector in the affine coordinate system

It can be easily seen that the following Lemma holds true:

Lemma 1. *The equations*

$$(4) \quad \begin{aligned} a_x &= \|\vec{a}\| \cos \alpha \\ a_y &= \|\vec{a}\| \cos \beta \\ a_z &= \|\vec{a}\| \cos \gamma \end{aligned}$$

are valid.

¹For the time being, let us think that the accelerometers measure correctly, i.e. a_x , a_y and a_z are the measured values from the accelerometers.

We want to express the affine projections \overline{a}_x , \overline{a}_y and \overline{a}_z of \vec{a} onto the coordinate axis with a_x , a_y and a_z .

Lemma 2. *For the affine projections of the acceleration \overline{a}_x , \overline{a}_y and \overline{a}_z the following equalities hold true:*

$$(5) \quad \begin{aligned} \overline{a}_x &= \frac{-\sin^2 \theta a_x + (\cos \phi - \cos \theta \cos \psi) a_y + (\cos \psi - \cos \phi \cos \theta) a_z}{-1 + \cos^2 \phi + \cos^2 \psi + \cos^2 \theta - 2 \cos \phi \cos \psi \cos \theta} \\ \overline{a}_y &= \frac{(\cos \phi - \cos \theta \cos \psi) a_x - \sin^2 \psi a_y + (\cos \theta - \cos \phi \cos \psi) a_z}{-1 + \cos^2 \phi + \cos^2 \psi + \cos^2 \theta - 2 \cos \phi \cos \psi \cos \theta} \\ \overline{a}_z &= \frac{(\cos \psi - \cos \phi \cos \theta) a_x + (\cos \theta - \cos \phi \cos \psi) a_y - \sin^2 \phi a_z}{-1 + \cos^2 \phi + \cos^2 \psi + \cos^2 \theta - 2 \cos \phi \cos \psi \cos \theta} \end{aligned}$$

Proof. We have

$$(6) \quad \vec{a} = \overline{a}_x \vec{e}_1 + \overline{a}_y \vec{e}_2 + \overline{a}_z \vec{e}_3,$$

where \vec{e}_1 , \vec{e}_2 and \vec{e}_3 are the unit vectors in the x , y and z directions, respectively. Consecutively, we take the scalar products of the both sides of (6) with \vec{e}_1 , \vec{e}_2 , \vec{e}_3 and obtain:

$$(7) \quad \begin{aligned} (\vec{a}, \vec{e}_1) &= \overline{a}_x + \overline{a}_y \cos \phi + \overline{a}_z \cos \psi \\ (\vec{a}, \vec{e}_2) &= \overline{a}_x \cos \phi + \overline{a}_y + \overline{a}_z \cos \theta \\ (\vec{a}, \vec{e}_3) &= \overline{a}_x \cos \psi + \overline{a}_y \cos \theta + \overline{a}_z \end{aligned}$$

Taking into account (4) we obtain

$$(8) \quad \begin{bmatrix} 1 & \cos \phi & \cos \psi \\ \cos \phi & 1 & \cos \theta \\ \cos \psi & \cos \theta & 1 \end{bmatrix} \begin{bmatrix} \overline{a}_x \\ \overline{a}_y \\ \overline{a}_z \end{bmatrix} = \begin{bmatrix} a_x \\ a_y \\ a_z \end{bmatrix}$$

We solve the system (8) and obtain (5). \square

Remark 1. Let us note that the system (8) has diagonally dominant matrix and, therefore, it has a unique solution.

Remark 2. In matrix form, equations (5) can be rewritten as

$$\overline{\mathbf{a}} = \overline{\mathbf{T}} \mathbf{a},$$

where:

$$\bar{\mathbf{a}} = \begin{bmatrix} \bar{a}_x \\ \bar{a}_y \\ \bar{a}_z \end{bmatrix},$$

$$\bar{T} = \frac{1}{den} \begin{bmatrix} -\sin^2 \theta & \cos \phi - \cos \theta \cos \psi & \cos \psi - \cos \phi \cos \theta \\ \cos \phi - \cos \theta \cos \psi & -\sin^2 \psi & \cos \theta - \cos \phi \cos \psi \\ \cos \psi - \cos \phi \cos \theta & \cos \theta - \cos \phi \cos \psi & -\sin^2 \phi \end{bmatrix},$$

$$den = -1 + \cos^2 \phi + \cos^2 \psi + \cos^2 \theta - 2 \cos \phi \cos \psi \cos \theta, \quad \mathbf{a} = \begin{bmatrix} a_x \\ a_y \\ a_z \end{bmatrix}$$

Lemma 2. For the acceleration $a_{nonorth}$ the following holds true

$$(9) \quad a_{nonorth} = \sqrt{\bar{a}_x^2 + \bar{a}_y^2 + \bar{a}_z^2 + 2\bar{a}_x\bar{a}_y \cos \phi + 2\bar{a}_x\bar{a}_z \cos \psi + 2\bar{a}_y\bar{a}_z \cos \theta}.$$

Proof. Taking $\mathbf{a} = a_{nonorth} = (\bar{a}_x, \bar{a}_y, \bar{a}_z)$ in (6) and taking the scalar squares of both sides, we obtain

$$(a_{nonorth}, a_{nonorth}) = \bar{a}_x^2 + \bar{a}_y^2 + \bar{a}_z^2 + 2\bar{a}_x\bar{a}_y(\vec{e}_1, \vec{e}_2) + 2\bar{a}_x\bar{a}_z(\vec{e}_1, \vec{e}_3) + 2\bar{a}_y\bar{a}_z(\vec{e}_2, \vec{e}_3),$$

where $\vec{e}_1, \vec{e}_2, \vec{e}_3$ are the unit vectors along the axis. Taking into account (3), (9) follows directly. \square

We substitute (5) into (9) and simplify to obtain the following:

Proposition 2. The equality

$$(10) \quad a_{nonorth} = \sqrt{\frac{numerator}{denominator}},$$

where

$$\begin{aligned} numerator = & 2(-1 + 1 \cos 2\theta)a_x^2 + 2(-1 + 1 \cos 2\psi)a_y^2 + 2(-1 + 1 \cos 2\phi)a_z^2 \\ & + 8(\cos \phi - \cos \psi \cos \theta)a_x a_y + 8(\cos \theta - \cos \phi \cos \psi)a_y a_z \\ & + 8(\cos \psi - \cos \phi \cos \theta)a_x a_z; \end{aligned}$$

$$denominator = 2 + 2 \cos 2\phi + 2 \cos 2\psi + 2 \cos 2\theta - 8 \cos \phi \cos \psi \cos \theta$$

holds true.

Now we shall derive an explicit expression for the calibrated values of the acceleration in an orthonormal coordinate system, given the data, measured by the sensors.

Proposition 3. Let $\vec{e}_1, \vec{e}_2, \vec{e}_3$ be the unit vectors in the directions, defined by the accelerometers' axis. Let us introduce an orthonormal coordinate system $O_{\vec{f}_1, \vec{f}_2, \vec{f}_3}$, where $\vec{f}_1 \equiv \vec{e}_1$, \vec{f}_2 is in the $\vec{e}_1\vec{e}_2$ plane. Then the following equality is valid:

$$(11) \quad \begin{bmatrix} \vec{e}_1 \\ \vec{e}_2 \\ \vec{e}_3 \end{bmatrix} = \overline{T}^{orth} \begin{bmatrix} \vec{f}_1 \\ \vec{f}_2 \\ \vec{f}_3 \end{bmatrix},$$

where

$$(12) \quad \overline{T}^{orth} = \begin{bmatrix} 1 & \cos \phi & \cos \psi \\ 0 & \sin \phi & \frac{\cos \theta - \cos \phi \cos \psi}{\sin \phi} \\ 0 & 0 & \frac{\sqrt{1 - \cos^2 \phi - \cos^2 \psi - \cos^2 \theta + 2 \cos \phi \cos \psi \cos \theta}}{\sin \phi} \end{bmatrix}$$

Proof. Let us denote (see Fig. 2)

$$\xi := \angle(\vec{e}_3, \vec{f}_2), \quad \eta := \angle(\vec{e}_3, \vec{f}_3).$$

Since \vec{f}_2 lies in the $\vec{e}_1\vec{e}_2$ plane and $\vec{f}_1 \equiv \vec{e}_1$ we have the relationship

$$(13) \quad \vec{e}_2 = b_1 \vec{f}_1 + b_2 \vec{f}_2,$$

where b_1 and b_2 are real numbers. By taking the inner product of (13) successively with \vec{f}_1 and \vec{f}_2 we obtain

$$b_1 = \cos \phi, \quad b_2 = \cos |90^\circ - \phi| = \sin \phi$$

Therefore, we have

$$\vec{e}_2 = \cos \phi \vec{f}_1 + \sin \phi \vec{f}_2$$

and, thus,

$$(14) \quad \vec{f}_2 = -\frac{\cos \phi}{\sin \phi} \vec{e}_1 + \frac{1}{\sin \phi} \vec{e}_2.$$

Analogously, we obtain

$$\vec{e}_3 = \cos \psi \vec{f}_1 + \cos \xi \vec{f}_2 + \cos \eta \vec{f}_3,$$

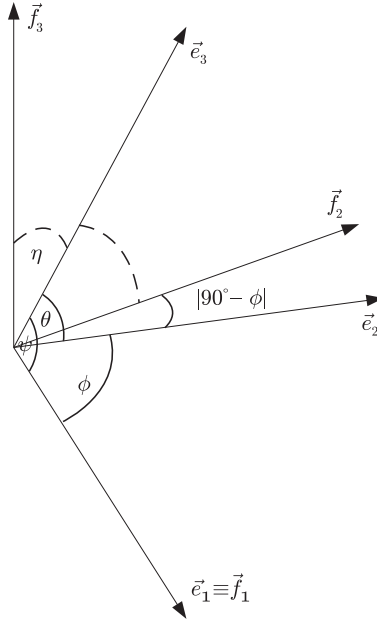


Figure 2: Orthonormal coordinate system

By taking into account (14), we obtain

$$\begin{aligned} \cos \xi &= \langle \vec{e}_3, \vec{f}_2 \rangle = \left\langle \vec{e}_3, -\frac{\cos \phi}{\sin \phi} \vec{e}_1 + \frac{1}{\sin \phi} \vec{e}_2 \right\rangle \\ &= -\frac{\cos \phi}{\sin \phi} \cos \psi + \frac{\cos \theta}{\sin \phi} = \frac{\cos \theta - \cos \phi \cos \psi}{\sin \phi}. \end{aligned}$$

Furthermore, since \vec{e}_3 is a vector in the orthonormal coordinate system $O_{\vec{f}_1 \vec{f}_2 \vec{f}_3}$ and the angles with the axis being ψ , ξ and η , respectively the following holds true:

$$\begin{aligned} \cos^2 \eta + \cos^2 \xi + \cos^2 \psi &= 1 \\ \cos \eta &= \sqrt{1 - \cos^2 \xi + \cos^2 \psi} \\ &= \frac{\sqrt{1 - \cos^2 \phi - \cos^2 \psi - \cos^2 \theta + 2 \cos \phi \cos \psi \cos \theta}}{\sin \phi} \end{aligned}$$

Let us note, that we have used the fact that η is small angle and, therefore, $\cos \eta > 0$. \square

Corollary 1. *Let us have an arbitrary acceleration \vec{a} with coordinates in the affine coordinate system $O_{\vec{e}_1 \vec{e}_2 \vec{e}_3}$, defined by the accelerometers' axis, \overline{a}_x , \overline{a}_y , \overline{a}_z ,*

respectively. Let the corresponding coordinates in the $O_{\vec{f}_1, \vec{f}_2, \vec{f}_3}$ coordinate system (defined as in Proposition 3) be \overline{a}_x^{orth} , \overline{a}_y^{orth} and \overline{a}_z^{orth} . Then we have

$$(15) \quad \begin{bmatrix} \overline{a}_x^{orth} \\ \overline{a}_y^{orth} \\ \overline{a}_z^{orth} \end{bmatrix} = \overline{T}^{orth} \begin{bmatrix} \overline{a}_x \\ \overline{a}_y \\ \overline{a}_z \end{bmatrix},$$

where \overline{T}^{orth} is defined as (12).

Let us denote

$$\overline{\mathbf{a}}^{orth} := \begin{bmatrix} \overline{a}_x^{orth} \\ \overline{a}_y^{orth} \\ \overline{a}_z^{orth} \end{bmatrix}, \quad \overline{\mathbf{a}} := \begin{bmatrix} \overline{a}_x \\ \overline{a}_y \\ \overline{a}_z \end{bmatrix}.$$

Furthermore, let us take into account (2), Remark 2 and Corollary 1 and the notation, introduced in those. Then we obtain the following important result:

Theorem 1. *Let \widehat{a}_x , \widehat{a}_y and \widehat{a}_z be the values shown by the accelerometers at a certain time and \overline{a}_x^{orth} , \overline{a}_y^{orth} and \overline{a}_z^{orth} be the coordinates of the corresponding acceleration in the orthonormal coordinate system, defined in Proposition 3. Then the following holds true:*

$$(16) \quad \overline{\mathbf{a}}^{orth} = \overline{T}^{orth} \overline{T} \widehat{\mathbf{a}} - \overline{T}^{orth} \overline{T} \mathbf{s}.$$

2.2. The calibration algorithm

Let us first note that when the device does not undergo any acceleration, then the length of the vector that the accelerometers should show is equal to the acceleration due to the gravitational force. The reason for this fact is that the accelerometers do not measure acceleration directly, but force. Now we are ready to explain the algorithm itself.

1. First, we make measurements with the three accelerometer sensors in 20 different positions, when the device does not undergo any acceleration. Let us denote those measurements with $\widehat{a}^{(i)}$, where $i = \overline{1, 20}$.
2. We make a ‘‘rough’’ estimate of the parameters in order to evaluate their signs. We achieve this by considering the simplified model, assuming the axis are orthogonal. Therefore, we find the values that minimize the sum

$$\sum_{i=1}^{20} \left[(T \widehat{a}^{(i)} - \mathbf{s})^T (T \widehat{a}^{(i)} - \mathbf{s}) - g^2 \right]^2$$

3. Using a least squares fit, we find the parameters in the model that minimize the sum

$$(17) \quad \sum_{i=1}^{20} \left[(\overline{T}^{orth} \overline{T} T \hat{a}^{(i)} - \overline{T}^{orth} \overline{T} s)^T (\overline{T}^{orth} \overline{T} T \hat{a}^{(i)} - \overline{T}^{orth} \overline{T} s) - g^2 \right]^2,$$

under the restrictions, imposed for the signs of the parameters by Step 2.

Let us note that Step 2 is important, because otherwise the numerical methods that we use for minimizing (17) do not always converge to the right values for the estimated parameters.

2.3. Estimates for the error due to nonorthogonality

We want to evaluate what is the error that can be caused by not considering the nonorthogonality of the axis. Let us denote

$$err(a_x, a_y, a_z, \phi, \psi, \theta) := |a_{nonorth} - a_{orth}|.$$

Since in the calibration procedure we use the fact that when the accelerometers are at rest, then the only acceleration that they measure is due to gravity, we consider the following extremal problem:

Problem 1.

$$(18) \quad \begin{aligned} err(a_x, a_y, a_z, \phi, \psi, \theta) &\longrightarrow \max, \\ a_{nonorth} &= g, \\ 0.98\pi &\leq \phi, \psi, \theta \leq 1.02\pi, \end{aligned}$$

where g is the gravitational acceleration.

Let us note that the restrictions for ϕ , ψ , θ are imposed because of the up to 2% nonorthogonality of the axis.

By solving this problem numerically, we obtain the estimate of the maximal error

$$\max err(a_x, a_y, a_z, \phi, \psi, \theta) \approx 0.3130299 \text{ m/s}^2$$

This value is reached, for example at

$$a_x = a_y = a_z \approx 5.48114, \phi = \psi = \theta \approx 1.60221$$

Next, we want to give an estimate for the upper bound of the relative error that can be reached when the accelerometer measures an arbitrary acceleration. We assume consecutively that in each direction the accelerometer can measure

acceleration up to $\pm 4g$, $\pm 8g$, $\pm 16g$. In all the cases the estimate is approximately the same.

Problem 2.

$$(19) \quad \begin{aligned} & \left| \frac{a_{nonorth} - a_{orth}}{a_{nonorth}} \right| \longrightarrow \max, \\ & -16g \leq a_x, a_y, a_z \leq 16g, \\ & 0.98\pi \leq \phi, \psi, \theta \leq 1.02\pi, \end{aligned}$$

The numerical solution of this extremal problem is approximately 3.192%.

Next, we present a histogram which represents the distribution of the relative error for values of ϕ , ψ , θ , respectively 1.53938, 1.60221, 1.60221, which are the estimated with the calibration procedure values for the sensor used in the tests (see Fig. 3).

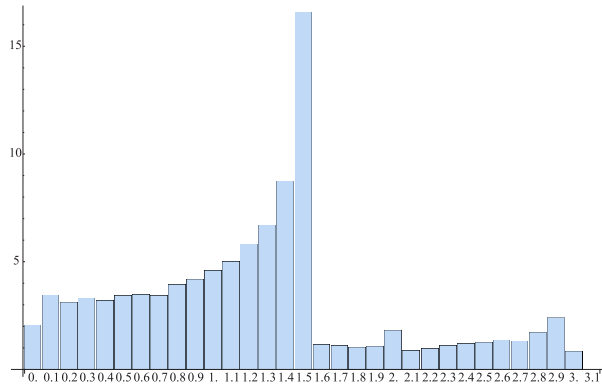


Figure 3: Distribution of the relative error

In order to be able to understand the “jump” in the histogram (Fig. 3), we present geometrically the domains in \mathbb{R}^3 where the relative error is respectively $\leq 1.4\%$, $\geq 1.4\%$, $\leq 1.6\%$, $\geq 1.6\%$ (see Fig.4). We assume again that ϕ , ψ , θ are, respectively 1.53938, 1.60221, 1.60221, and a_x , a_y , a_z lie in the interval $[-20, 20]$.

All of those results show that the error that is due to the non-orthogonality of the axis is very serious one and cannot be neglected in order to obtain a linear model for the acceleration.

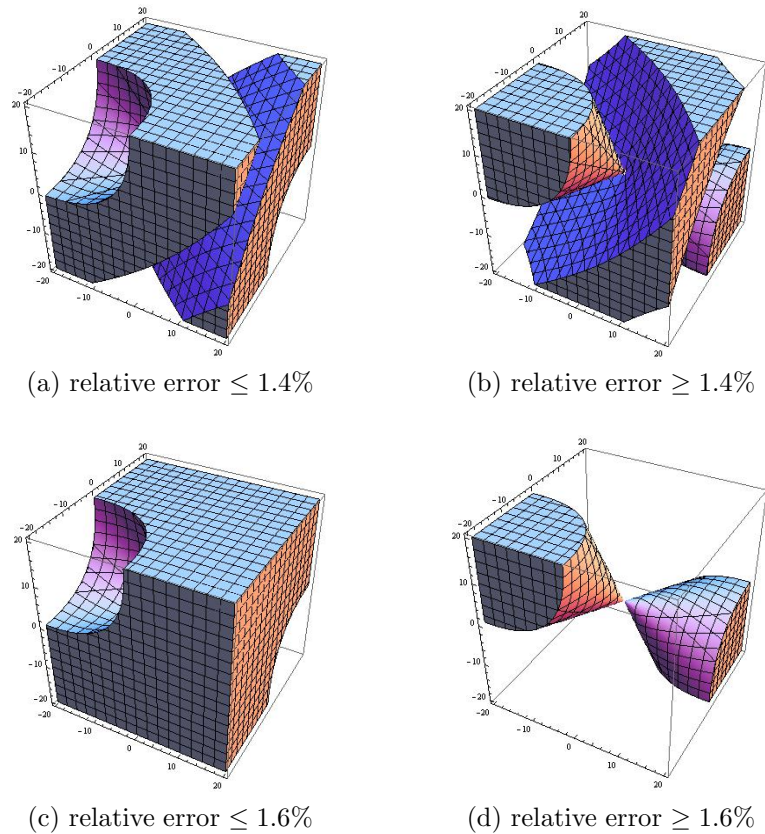


Figure 4: Domains in \mathbb{R}^3 for the relative error

2.4. Conducted experiments

In this subsection we present some experiments, that we have conducted in order to test the algorithm that we propose. We have tested it with 3 datasets from 3 different phones, each consisting of averaged measurements of the sensors in 27 different positions when the device does not undergo any acceleration. We have used 20 of those positions for calibrating the device and the other 7 we have used to check the results, by comparing the already calibrated acceleration with g .

- **Dataset 1.** In Table 1 the measured data from the three accelerometer sensors is shown.

– First, we calibrate the device, using positions 1–20, i.e. we find the

Position	x	y	z
1	-9.54983	0.37829	-0.999283
2	10.145	0.314528	-1.37789
3	0.413309	-9.47641	-1.62076
4	0.368766	10.1442	-0.910232
5	0.510292	0.338026	-10.7851
6	0.231834	0.482186	8.60553
7	0.230219	7.85729	5.09836
8	0.304598	8.0554	-7.09352
9	-0.612011	-7.07391	-7.39908
10	-0.741095	-7.0657	5.22667
11	8.34517	-1.00171	4.35023
12	7.90356	-1.01121	-7.15935
13	-7.21644	-0.678396	5.06995
14	-7.53767	-0.887223	-6.8451
15	0.359915	1.36831	8.5543
16	0.0692607	1.56694	-10.7058
17	0.491484	-0.827214	8.55852
18	0.0425242	-0.802927	-10.712
19	-1.00027	0.562196	-10.6961
20	1.765	0.425372	8.51681
21	-1.90224	7.05	5.60731
22	2.7946	7.32034	-7.46149
23	-6.09005	-5.89288	2.99988
24	-6.12614	-2.40266	-7.91477
25	-5.17908	-5.64109	4.39876
26	-6.40025	7.4125	0.119649
27	-2.75267	7.19283	5.10852

Table 1: Dataset 1

values of the parameters, that minimize the sum

$$\sum_{i=1}^{20} \left[(\overline{T}^{orth} \overline{T} T \hat{a}^{(i)} - \overline{T}^{orth} \overline{T} s)^T (\overline{T}^{orth} \overline{T} T \hat{a}^{(i)} - \overline{T}^{orth} \overline{T} s) - g^2 \right]^2,$$

where $\hat{a}^{(i)}$ is the vector, consisting of the measurements in the i -th position in Table 1. We obtain the following values for the calibration

parameters:

$$\begin{aligned} s_1 &\rightarrow 0.304496, s_2 \rightarrow 0.321482, s_3 \rightarrow -1.08995, \\ b_1 &\rightarrow -1.00457, b_2 \rightarrow -1.00147, b_3 \rightarrow -0.989292, \\ \phi &\rightarrow 1.57646, \psi \rightarrow 1.57096, \theta \rightarrow 1.57301 \end{aligned}$$

– Analogously, using positions 3–23, we obtain:

$$\begin{aligned} s_1 &\rightarrow 0.318321, s_2 \rightarrow 0.322794, s_3 \rightarrow -1.09059, \\ b_1 &\rightarrow -1.00472, b_2 \rightarrow -1.00124, b_3 \rightarrow -0.989255, \\ \phi &\rightarrow 1.56932, \psi \rightarrow 1.5709, \theta \rightarrow 1.57296 \end{aligned}$$

Using the obtained values for the calibration parameters, we evaluate the relative error over all measured positions, i.e. we estimate

$$\left| \frac{a - g}{g} \right|,$$

where a is the absolute value of the acceleration, calculated with formula (16). In all cases it is less than 0.21%.

- **Dataset 2.** In Table 2 the measured data from the three accelerometer sensors from the second device is shown.

– Using positions 1–20, we obtain:

$$\begin{aligned} s_1 &\rightarrow -0.469784, s_2 \rightarrow 0.608425, s_3 \rightarrow 0.208206, \\ b_1 &\rightarrow -0.999573, b_2 \rightarrow -0.989443, b_3 \rightarrow -1.01176, \\ \phi &\rightarrow 1.56219, \psi \rightarrow 1.56969, \theta \rightarrow 1.57057 \end{aligned}$$

– Using positions 3–23, the estimated values are:

$$\begin{aligned} s_1 &\rightarrow -0.466405, s_2 \rightarrow 0.616422, s_3 \rightarrow 0.207149, \\ b_1 &\rightarrow -0.999212, b_2 \rightarrow -0.989644, b_3 \rightarrow -1.01181, \\ \phi &\rightarrow 1.55782, \psi \rightarrow 1.56827, \theta \rightarrow 1.57215 \end{aligned}$$

Once again, the values are very close to one another. The worst relative error that is reached with those calibrations is below 0.45%.

Position	x	y	z
1	7.324190906	1.250997715	-5.785632422
2	-8.334818875	1.423071223	6.075933722
3	-0.55309323	-1.556750779	-9.465058152
4	0.3963949	-2.401782608	9.590842176
5	4.468067668	0.438564599	8.815483348
6	-0.25604359	-8.251388776	4.231704803
7	-10.19639516	-0.540933147	-0.043947822
8	9.243301882	-0.489659084	0.177376713
9	5.184601909	0.464227916	-7.888789547
10	-7.133046458	0.486715023	7.492167273
11	-3.544315793	-5.885572603	-6.514445229
12	1.927551054	-5.721122639	7.317886686
13	0.712132815	0.611587605	10.05427574
14	-0.516080232	-1.053660856	-9.563502952
15	-0.482513916	-0.519767116	10.04926657
16	-0.366261687	1.69466758	-9.659420825
17	-1.770079301	0.62190275	10.02684107
18	0.714671068	0.553163819	-9.626586644
19	-0.557896244	1.798565701	10.05206135
20	-0.633628967	7.907637143	6.736185309
21	-0.244376238	7.911662259	-6.344980284
22	-0.391871362	-6.71082086	-6.278043744
23	-1.109805182	-6.966091847	6.382627512
24	-10.2685151	0.6944625	0.553426001
25	9.263098671	0.708257972	1.16414443
26	-0.341591276	-9.051813894	0.526102398
27	-0.766906823	10.32812321	0.883673299
28	0.139849901	0.372395084	-9.689413968
29	-0.825407808	0.440694427	10.10000846

Table 2: Dataset 2

- **Dataset 3.** In the last dataset, shown in Table 3, it is important to note, that the measurements from positions 3 and 21 are very similar to each other. As one can see from the results shown below, if we use both those position for calibration purposes the result is much worse.
 - Using positions 1–20 (i.e. using only one of the similar rows of data), we obtain a relative error of 0.26%
 - Using positions 3–23, we obtain a relative error of 0.98%

This shows that it is important to make the measurements in distinct po-

Position	x	y	z
1	0.686143985	9.693013241	0.146230973
2	0.307313184	-9.555131822	0.121707371
3	10.20588166	0.146627372	0.293913142
4	-9.235730337	0.149835656	-0.153514714
5	0.277144172	-0.108499369	9.72381854
6	0.652333397	0.026782191	-9.867581581
7	2.819218128	0.00984892	9.453752615
8	-1.006468208	0.586054944	9.610065897
9	10.10396889	0.089937928	-1.625049867
10	-1.605962585	0.058272144	-9.639987664
11	0.246794337	1.126126555	9.709396155
12	0.706211903	-3.139230967	-9.302827738
13	7.728566894	0.248629672	6.471431237
14	2.053861069	-2.927665847	9.11283197
15	5.742237957	0.041531765	8.152279472
16	1.604557037	0.951821853	-9.754449668
17	1.029262184	1.996550095	9.543562547
18	0.041407842	-2.516368282	9.358991009
19	2.730162016	-8.137597633	-4.711984149
20	-2.924918942	-6.411393964	6.335544161
21	10.18267071	0.144573621	0.312617999
22	3.908533423	-8.83618239	-1.558956159
23	-4.59854197	-8.151722848	0.065404421
24	-1.674747469	9.466063897	0.036135226
25	10.04636598	1.799748205	0.246702889
26	7.685992297	6.529638446	0.083514447

Table 3: Dataset 3

sitions. Otherwise, the least-squares fit is biased towards one position and the result gets worse.

2.5. Conclusion

We have derived an explicit formula for the linear acceleration, given the values of the accelerometers and the angles between the axis of the sensors. We have explained how one can find an approximation of those angles and the shifts and scaling coefficients, given some measurements of the sensors, when the system does not undergo any acceleration. We have run some numerical experiments in order to understand better the error, caused by the nonorthogonality of the axis.

Future work on the topic could include studying the error with which the calibration parameters are evaluated with the procedure that we propose. Also,

the optimal positions in which the calibration data is to be collected, should be determined. Probably, more investigation on the errors can give some insights about those positions.

3. Approach 2

This approach was studied by Irina Georgieva and Clemens Hofreither.

3.1. Mathematical problem description

We are concerned with an end-user device (e.g., smart phone) with a built-in accelerometer which measures accelerations along three axes. In the following, we refer to the true acceleration which acts on the device by a , and to the measurements which its sensor outputs by m .

In practice, the measurements m will not coincide with the true physical acceleration a due to many factors, among these,

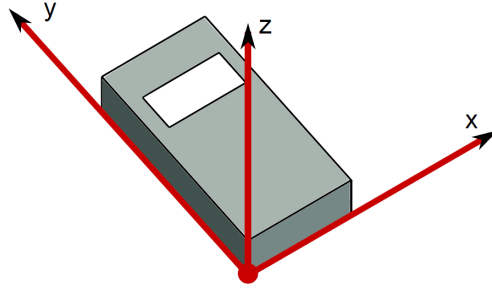
- scaling errors,
- crosstalk,
- offset errors,
- non-orthogonality of the accelerometer axes,
- time-dependent noise,
- etc.

We want to find and calibrate a model which allows us to reconstruct as well as possible the true accelerations from the measured data,

$$m \mapsto a,$$

by taking into account the systematic errors in the accelerometer of one particular device.

For all further considerations, we fix a coordinate system relative to the phone as shown in the below picture.



All accelerations a

$$a = (a_x, a_y, a_z)$$

acting on the phone will be considered in this coordinate system. We point out that this coordinate system may not be aligned with the axes of the accelerometer, and there is no need for this.

3.2. Mathematical model

We assume an affine-linear relationship between the measurements $m = (m_1, m_2, m_3)$ and the true acceleration vector $a = (a_1, a_2, a_3)$, that is, the function $m = F(a)$ should be of the form

$$m = F(a) = Xa + y.$$

Here, $X \in \mathbb{R}^{3 \times 3}$ is an unknown matrix, and $y \in \mathbb{R}^3$ is an unknown vector. In this model, the diagonal of X may represent the scaling error, the off-diagonal entries of X the crosstalk factors, and y the offset. However, X can also represent arbitrary rotations in the case that the accelerometer sensor is not installed in an axis-aligned way in the device.

Once we have computed X and y , we can simply invert the above formula to obtain the true acceleration a from measurements m by the formula

$$(20) \quad a = F^{-1}(m) = X^{-1}(m - y).$$

This model has 12 parameters, namely, the 9 entries of X plus the 3 entries of y .

3.3. Determining the parameters

Let us assume that we have put the device into a standard orientation for which the actual forces a which act on it are known. For instance, putting the device facing up on a flat table, we can assume that the force is

$$a = (0, 0, -g),$$

where $g \approx 9.81 \text{ m/s}^2$ is the gravitational acceleration. By reading the output of the sensor and averaging over a sufficiently long span of time in order to reduce the measurement noise, we obtain a measured acceleration $m = (m_1, m_2, m_3)$.

By our model, we know that

$$Xa + y = m,$$

or in component form,

$$\begin{aligned} x_{11}a_1 + x_{12}a_2 + x_{13}a_3 + y_1 &= m_1, \\ x_{21}a_1 + x_{22}a_2 + x_{23}a_3 + y_2 &= m_2, \\ x_{31}a_1 + x_{32}a_2 + x_{33}a_3 + y_3 &= m_3. \end{aligned}$$

Remember that X and y are unknown, and we collect all their components into a single vector $z \in \mathbb{R}^{12}$ of unknowns,

$$(21) \quad z = (x_{11}, x_{12}, x_{13}, x_{21}, x_{22}, x_{23}, x_{31}, x_{32}, x_{33}, y_1, y_2, y_3)^\top,$$

for which we want to solve. Rewriting the above three equations in matrix-vector form, we obtain

$$\begin{pmatrix} a_1 & a_2 & a_3 & 0 & 0 & 0 & 0 & 0 & 0 & 1 & 0 & 0 \\ 0 & 0 & 0 & a_1 & a_2 & a_3 & 0 & 0 & 0 & 0 & 1 & 0 \\ 0 & 0 & 0 & 0 & 0 & 0 & a_1 & a_2 & a_3 & 0 & 0 & 1 \end{pmatrix} z = m.$$

Denoting the matrix in the above equation by $K(a) \in \mathbb{R}^{3 \times 12}$, we can shortly write

$$K(a)z = m.$$

However, this system of linear equations has 12 unknowns, but only 3 equations and is therefore underdetermined.

In order to get a solution, we need to make a series of N measurements m for different known accelerations a . We will denote them by

$$\begin{aligned} a^{(1)} &= (a_1^{(1)}, a_2^{(1)}, a_3^{(1)}), & m^{(1)} &= (m_1^{(1)}, m_2^{(1)}, m_3^{(1)}), \\ & & \vdots & \\ a^{(N)} &= (a_1^{(N)}, a_2^{(N)}, a_3^{(N)}), & m^{(N)} &= (m_1^{(N)}, m_2^{(N)}, m_3^{(N)}). \end{aligned}$$

Setting up the linear system we have derived above for each of these measurements, we get a complete linear system of the form

$$\begin{bmatrix} K(a^{(1)}) \\ K(a^{(2)}) \\ \vdots \\ K(a^{(N)}) \end{bmatrix} z = \begin{bmatrix} m^{(1)} \\ m^{(2)} \\ \vdots \\ m^{(N)} \end{bmatrix}.$$

We call the block matrix on the left-hand side K and observe that it has size $3N \times 12$, and call \bar{m} the right-hand side vector of size $3N$. In short, we have the linear system

$$Kz = \bar{m}.$$

If we take $N = 4$ measurements, the system is square, and it is uniquely solvable provided that the four vectors

$$(22) \quad \left(a_1^{(i)}, a_2^{(i)}, a_3^{(i)}, 1 \right), \quad i = 1, 2, 3, 4$$

are linearly independent.

In practice, we recommend taking more measurements, say, at least $N = 6$ by measuring all six canonical orientations of a box-shaped device. The resulting linear system is then overdetermined. By using the standard technique of least-squares fitting, we can pass to the square linear system

$$K^\top Kz = K^\top \bar{m}$$

which gives us the unique minimizer of

$$|\bar{m} - Kz|^2.$$

Again, this system has a unique solution provided that any four vectors from $\{a^{(i)}\}$ satisfy the linear independence condition from (22).

The matrix $K^\top K$ has size 12×12 and can thus easily and quickly be inverted by standard linear solvers, for instance, Gaussian elimination.

Once we have solved this linear system and obtained z , we can refer to formula (21) and simply extract the coefficients to obtain the original matrix X and the vector y . Then, from formula (20), we get the relation which allows us to compute the true accelerations a from arbitrary measurements m .

3.3.1. Simplification of the least-squares system

In practice, it is a very natural choice to have the known accelerations point along the positive and negative coordinate axes, i.e.,

$$\begin{aligned} a^{(1)} &= (-g, 0, 0), & a^{(3)} &= (0, -g, 0), & a^{(5)} &= (0, 0, -g), \\ a^{(2)} &= (g, 0, 0), & a^{(4)} &= (0, g, 0), & a^{(6)} &= (0, 0, g). \end{aligned}$$

In Subsection 3.4, we show how to obtain these measurements in a simple way. For this natural choice, it is easy to see that the least-squares matrix takes the form of a diagonal matrix, namely,

$$K^\top K = \text{diag}(2g^2, 2g^2, 2g^2, 2g^2, 2g^2, 2g^2, 2g^2, 2g^2, 6, 6, 6).$$

Therefore, in this case, the least-squares problem

$$K^\top K z = K^\top \bar{m}$$

admits a simple solution in closed form,

$$\begin{aligned} X &= \frac{1}{2g} \begin{pmatrix} -m_1^{(1)} + m_1^{(2)} & -m_1^{(3)} + m_1^{(4)} & -m_1^{(5)} + m_1^{(6)} \\ -m_2^{(1)} + m_2^{(2)} & -m_2^{(3)} + m_2^{(4)} & -m_2^{(5)} + m_2^{(6)} \\ -m_3^{(1)} + m_3^{(2)} & -m_3^{(3)} + m_3^{(4)} & -m_3^{(5)} + m_3^{(6)} \end{pmatrix}, \\ y &= \frac{1}{6} \sum_{i=1}^6 m^{(i)}. \end{aligned}$$

Therefore, in this case, it is no longer required to invert a matrix for the calibration. Instead, only very few arithmetic operations on the measured data are needed, which is very computationally cheap and can be done without extra software on the user device itself.

3.4. Calibration procedure

We propose a simple method for obtaining six different measurements in six canonical orientations of the user device. This procedure depends on the assumption that the device is roughly box-shaped. If this is not the case, it has to be held in place with a suitable construction.

For this procedure, we simply have the user put the device in its six standard positions. In order to keep the device well-oriented and stable, simple everyday objects like window frames or bookshelves can be used. In a laboratory setting, nivellation of the involved surface can be performed beforehand to increase the accuracy.

In each of the six positions, the accelerometer output will be measured for a few seconds and then averaged in order to reduce the measurement noise. This finally gives us six vectors $m^{(1)}, \dots, m^{(6)}$ with known true accelerations $a^{(1)}, \dots, a^{(6)}$ resulting from Earth gravity.

An example of how the procedure can be performed is shown in the pictures below.



3.5. Examples

We were given two example datasets taken from two different devices and ran our method on this input data. One more dataset was captured by ourselves in order to test the calibration procedure. In the following, we describe the results of these experiments.

3.5.1. Example: Huawei

We have 29 accelerations $m^{(i)}$ which were measured in different positions. From these, the first six,

$$\begin{array}{ccc} -9.54983 & 0.37829 & -0.999283 \\ 10.145 & 0.314528 & -1.37789 \\ 0.413309 & -9.47641 & -1.62076 \\ 0.368766 & 10.1442 & -0.910232 \\ 0.510292 & 0.338026 & -10.7851 \\ 0.231834 & 0.482186 & 8.60553 \\ \vdots & \vdots & \vdots \end{array}$$

are known to have been taken in the six standard positions described in Subsection 3.4. Our algorithm computes the model parameters

$$X = \begin{pmatrix} 1.00381 & -0.00227028 & -0.0141925 \\ -0.00324982 & 1.00003 & 0.00734762 \\ -0.019297 & 0.0362144 & 0.988311 \end{pmatrix},$$

$$y = \begin{pmatrix} 0.353222 \\ 0.363473 \\ -1.18129 \end{pmatrix}.$$

We point out that the computed offset errors y are within the tolerances from the sensor data sheet [5] that we were provided with, namely, $\pm 0.49 \text{ m/s}^2$ for the x and y axes and $\pm 1.96 \text{ m/s}^2$ for the z axis.

In order to determine how well the linear model fits the given data, we compute the relative fitting error for the first six measurements,

$$\max_{i=1,\dots,6} \frac{\|F^{-1}(m^{(i)}) - a^{(i)}\|}{\|a^{(i)}\|} = 0.010601.$$

If one computes the same errors based on the raw measurements, one finds a much larger error,

$$\max_{i=1,\dots,6} \frac{\|m^{(i)} - a^{(i)}\|}{\|a^{(i)}\|} = 0.17386.$$

The observed improvement after calibration is therefore about 16.4 times.

For the remaining measurements, we do not know the true accelerations. However, we know that they were taken in stationary positions and thus their norms should be g . After calibration, the maximum relative error in the norms is

$$\max_{i=1,\dots,29} \frac{|\|F^{-1}(m^{(i)})\| - g|}{g} = 0.0315425,$$

whereas for the original data we have

$$\max_{i=1,\dots,29} \frac{|\|m^{(i)}\| - g|}{g} = 0.122075.$$

Here the improvement is about 3.87 times.

3.5.2. Example: GT

For a second dataset labelled “GT”, we were given 27 measurements where again the first six were used to calibrate the device. For this data, the algorithm computed the parameters

$$X = \begin{pmatrix} 0.990908 & 0.0193084 & -0.0191228 \\ -0.000163521 & 0.981047 & -0.00689508 \\ 0.0228047 & 0.00124993 & 0.998542 \end{pmatrix},$$

$$y = \begin{pmatrix} 0.482181 \\ 0.0587712 \\ 0.0440956 \end{pmatrix}.$$

The obtained offset errors are noticeably smaller than in the first example, indicating that this device has more accurate sensors or was better calibrated already in the factory.

As in the previous example, we compute the calibration error

$$\max_{i=1,\dots,6} \frac{\|F^{-1}(m^{(i)}) - a^{(i)}\|}{\|a^{(i)}\|} = 0.0158458$$

and compare it to the original sensor data,

$$\max_{i=1,\dots,6} \frac{\|m^{(i)} - a^{(i)}\|}{\|a^{(i)}\|} = 0.0725016.$$

The improvement is about 4.58 times.

We also again compute the relative errors in the norms,

$$\max_{i=1,\dots,27} \frac{|\|F^{-1}(m^{(i)})\| - g|}{g} = 0.0138985,$$

and compare it to the original data,

$$\max_{i=1,\dots,27} \frac{|\|m^{(i)}\| - g|}{g} = 0.0582853.$$

The improvement is about 4.19 times.

3.5.3. Test of robustness of calibration procedure

As suggested by our industry partner, we have compared the results of several calibration runs. For this, we took 20 measurements of five seconds each in each of the six standard positions with another Huawei phone, giving us 20 independent datasets with which we can perform calibration.

The mean of the model parameters over the 20 trials is

$$\begin{pmatrix} 1.00367 & -0.00200432 & 0.0211193 \\ 0.00396457 & 1.00055 & -0.00489847 \\ 0.00346578 & 0.00534244 & 0.989011 \end{pmatrix}, \begin{pmatrix} 0.264937 \\ 0.418299 \\ -1.1462 \end{pmatrix}.$$

The standard deviations of the model parameters over these 20 trials are

$$\begin{pmatrix} 0.00021274 & 0.0016114 & 0.000203203 \\ 0.00109465 & 0.000171741 & 0.000251313 \\ 0.000307081 & 0.000715155 & 0.000315258 \end{pmatrix}, \begin{pmatrix} 0.00439571 \\ 0.00300421 \\ 0.00463018 \end{pmatrix}.$$

These deviations are well below the magnitudes of the obtained model parameters, which indicates that repeated calibration runs should generally result in very similar calibration parameters. In other words, the calibration procedure seems to be quite robust.

3.6. Conclusions

We have presented a calibration method which

- is easy to implement,
- requires only simple measurements which the end user can perform in a few minutes using no extra tools,
- is computationally very cheap,
- significantly reduces the error on the tested data sets,
- allows the reconstruction of the true accelerations in a known coordinate system,
- results in a model which remains valid in the non-stationary case.

Acknowledgment

The authors would like to express their sincere gratitude to Assoc. Prof. Kiril Alexiev and to Angel Ivanov – a representative of MM Solutions AD for their time and valuable advices, that have helped the present work a lot.

References

- [1] Chatfield, A.B.: Fundamentals of High Accuracy Inertial Navigation, volume 174 of Progress in astronautics and aeronautics. American Institute of Aeronautics and Astronautics, Reston, VA, USA, 1997.
- [2] Forsberg, T., Grip, N., Sabourova, N.: Non-Iterative Calibration for Accelerometers with Three Non-Orthogonal Axes and Cross-Axis Interference. Research Report No. 8, Department of Engineering Sciences and Mathematics, Division of Mathematics, Lulea University of Technology, 2012.
- [3] Grip, N., Sabourova, N.: Simple Non-Iterative Calibration for Triaxial Accelerometers. Research Report No. 7, Department of Engineering Sciences and Mathematics, Division of Mathematics, Lulea University of Technology, 2011.
- [4] Woodman, O.: An introduction to inertial navigation. Technical reports published by the University of Cambridge. ISSN 1476-2986. (2007)
- [5] MPU-6000 and MPU-6050 Product Specification Revision 1.0. InvenSense Inc. (2010)